# Pharmacophoric features of *Pseudomonas aeruginosa* deacetylase LpxC inhibitors: An electronic and structural analysis

Rameshwar U. Kadam, Archana Chavan and Nilanjan Roy*

*Center of Pharmacoinformatics, National Institute of Pharmaceutical Education and Research,
Sector 67, S.A.S. Nagar, Punjab 160 062, India*

**Abstract**—Various electronic properties of structurally diverse synthetic LpxC inhibitors containing oxazoline, aroylserine and thiazoline rings were calculated and correlated with biological activity. These electronic features include the magnitude and locations of 3-dimensional molecular electrostatic potentials, hydrogen bond acceptor/donor density, lowest unoccupied molecular orbital, and highest occupied molecular orbital. Strong correlation of these stereo-electronic properties with LpxC inhibitory potency reveals the potential pharmacophoric features of specific LpxC inhibitors. Thus, these pharmacophoric features of LpxC inhibitors based on electronic and surface analysis could be successfully exploited for designing more potent LpxC inhibitors.
© 2006 Elsevier Ltd. All rights reserved.

Recently, the resistance developed by different Gram-negative bacterial species to antibiotics such as beta-lactams (tacarcillin, carbapenem (e.g., imipenem-cilastatin, meropenem), aminoglycoside (tobramycin), ceftazidime, carbapenem (e.g., imipenem-cilastatin, meropenem), etc.) substantiates the need of identification and development of novel anti-bacterial targets[1,2] (http://www.emedicine.com/med/topic1943.htm). This search led to identification and characterization of UDP-3-*O*-[*R*-3-hydroxymyristoyl]-GlcNAc deacetylase (LpxC), as an attractive target against *Pseudomonas* and other Gram-negative bacterial species infection. UDP-{3-*O*-[(*R*)-3-hydroxymyristoyl]}-*N*-acetylglucosamine deacetylase (LpxC) is a metal-dependent deacetylase, which catalyzes the first committed step in lipid A biosynthesis by hydrolyzing UDP-{3-*O*-[(*R*)-3-hydroxymyristoyl]}-*N*-acetylglucosamine to form acetate and UDP-{3-*O*-[(*R*)-3-hydroxymyristoyl]}-glucosamine. This step serves as a permeability barrier that protects the bacterium from antibiotics.[3]

Untill date, the inhibitors developed against LpxC enzymes of different Gram-negative bacteria contain hydroxamate or phosphonate zinc-binding motifs.[4,5] Most compounds reported to date are not selective for

*Pseudomonas aeruginosa* LpxC and detailed SAR are not reported for these inhibitors. Thus, determining molecular electronic properties responsible for LpxC inhibitory potency should lead toward a better understanding of inhibitor-enzyme action and aid in the designing of potent LpxC inhibitors. Interactions between molecules are a consequence of stereo-electronic interactions, that is, it is the molecule's stereo-electronic properties that govern strength of bonds, strength of non-bonded interactions, and molecular reactivity. Molecular electronic properties affect the strength of interaction with receptor proteins and transport across cell membranes.

The present study explains the structural diversity of the LpxC inhibitors (Table 1) by determining how ring type, cyclic versus acyclic groups, and presence of stereo-centers affect their molecular electronic properties. The results show that all of these structurally diverse compounds share specific electronic properties. The heterocyclic ring compounds are slightly different than the non-heterocyclic ring compounds with respect to the nucleophilicity of their nitrogen and the electrophilicity of their hydroxyl group. These differences may indicate different strengths of interaction with receptors.

The LpxC inhibitors reported by Kline et al. were used for this study.[4] The 28 compounds were selected from dataset of 63 compounds on the basis of known stereochemistry. The compounds with percentage

**Table 1.** Structures, activities, and theoretical value of MESP and HD for 2-Aryloxazolines, Aroylserines (A), and 2-Arylthiazolines (B)



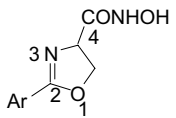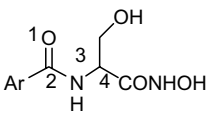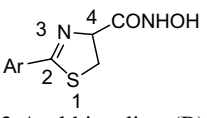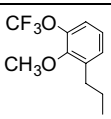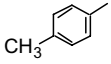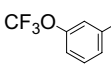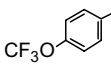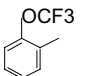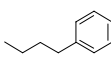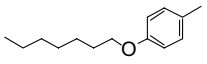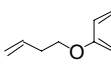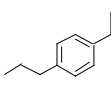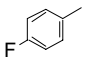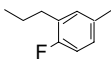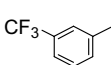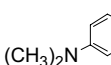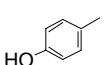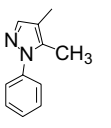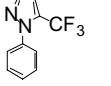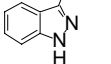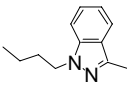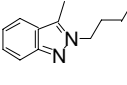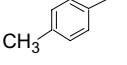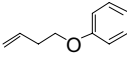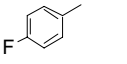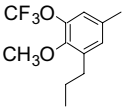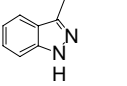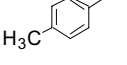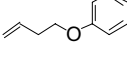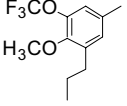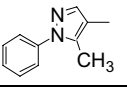2-Aryloxazolines          Aroylserines (A)          2-Arylthiazolines(B)

| Mol. I.D. | Ar | $IC_{50}$ | Most negative potential[a] | Most positive potential[a] | HD[a1] (high) | HD[a1] (low) |
|---|---|---|---|---|---|---|
| 5 | CF$_3$O, CH$_3$O (propyl benzene) | 0.5 | −52.0 | 32.6 | 0.109 | 0.000 |
| 19b | CH$_3$ (dimethyl benzene) | 20 | −52.1 | 34.2 | 0.109 | 0.000 |
| 25 | CF$_3$O (methyl benzene) | 6.0 | −50.0 | 37.5 | 0.110 | 0.000 |
| 26 | CF$_3$O (methyl benzene) | 5.0 | −53.1 | 33.8 | 0.108 | 0.016 |
| 28 | OCF3 (methyl benzene) | >10 | −56.9 | 31.6 | 0.107 | 0.000 |
| 29 | butyl methyl benzene | 7.3 | −51.6 | 35.4 | 0.108 | 0.019 |
| 30 | hexyloxy methyl benzene | >30 | −57.6 | 30.4 | 0.108 | 0.000 |
| 31 | allyloxy methyl benzene | 5.6 | −51.3 | 34.1 | 0.108 | 0.000 |
| 32 | propyl biphenyl methyl | 0.28 | −50.6 | 36.3 | 0.108 | 0.000 |
| 35 | F, methyl benzene | 6.0 | −50.5 | 37.8 | 0.107 | 0.013 |
| 38 | propyl F methyl benzene | 0.96 | −50.2 | 37.6 | 0.109 | 0.000 |
| 47 | CF$_3$ methyl benzene | 2.5 | −49.0 | 44.3 | 0.109 | 0.000 |
| 52 | (CH$_3$)$_2$N methyl benzene | 4.9 | −56.8 | 32.1 | 0.108 | 0.011 |
| 53 | HO methyl benzene | >30 | −57.4 | 43.5 | 0.108 | 0.016 |
| 58 | N,N pyrazole CH$_3$ phenyl | >30 | −60.9 | 36.6 | 0.106 | 0.000 |
| 59 | N,N pyrazole CF$_3$ phenyl | >30 | −54.5 | 40.1 | 0.109 | 0.000 |
| 60 | methyl indazole N NH | 5.5 | −52.0 | 47.5 | 0.108 | 0.000 |

**Table 1** (*continued*)

| Mol. I.D. | Ar | IC$_{50}$ | Most negative potential[a] | Most positive potential[a] | HD[a1] (high) | HD[a1] (low) |
|---|---|---|---|---|---|---|
| 61 | | 10 | −52.1 | 29.7 | 0.108 | 0.000 |
| 62 | | 12 | −49.8 | 33.0 | 0.093 | 0.000 |
| 65[A] | CH$_3$ | >50 | −53.3 | 61.4 | 0.111 | 0.000 |
| 66[A] | | 3.9 | −47.9 | 49.4 | 0.111 | 0.000 |
| 67[A] | F | >50 | −51.2 | 57.8 | 0.113 | 0.012 |
| 71[A] | CF$_3$O, CH$_3$O | >50 | −53.8 | 56.3 | 0.111 | 0.000 |
| 72[A] | | 13 | −49.8 | 50.6 | 0.110 | 0.000 |
| 76[B] | H$_3$C | 38.5 | −44.3 | 47.0 | 0.110 | 0.000 |
| 77[B] | | 58.7 | −53.2 | 33.6 | 0.109 | 0.000 |
| 80[B] | F$_3$CO, H$_3$CO | 17.8 | −53.6 | 29.7 | 0.109 | 0.000 |
| 81[B] | CH$_3$ | >60 | −59.3 | 32.3 | 0.105 | 0.000 |

(A) Indicate aroylserines series and (B) indicate 2-arylthiazolines series and remaining are 2-aryloxazolines series.
[a] Indicate (kcal/mol) unit.
[a1] Indicate (e/au$^2$) unit.

enantiomeric purity of <95% and racemates were removed from the study taking into consideration the R-configuration at 4-position in ring (a chiral center [(–C(=O)–NH(OH))] (Table 1)). The ligands under study were built by keeping constraint on restricted rotation about amide bond [(–C(=O)–NH(OH))] using SYBYL6.9 molecular modeling package installed on a Silicon Graphics Fuel Work station running IRIX 6.5 operating system.[6] Since the ligand-bound crystal structure of *P. aeruginosa* LpxC is not known, the potent molecule with known configuration in LpxC inhibitor series was selected (i.e., molecule 32).[4] The systematic conformation search procedure in SYBYL6.9. was implemented to find out lowest energy conformation for molecule **32** and subsequently, minimized using PM3 Hamiltonian using MOPAC interfaced with SYBYL6.9. In order to generate accurate charge information a single-point energy calculation was also performed using the AM1 Hamiltonian[7] on the PM3 optimized geometry. Thereafter, the geome-

try structure of molecule **32** was used to analyze the bond lengths and dihedral angles (Supplementary material 1, Fig. 1a and b). Molecule **32** is a biphenyl linked at 3-position of oxazoline moiety and makes a dihedral angle ($\theta_2$) of −175.4° between the phenyl ring and oxazoline moiety. Moreover it is a conjugated molecule because most bond lengths of C–C are in the range of 1.39–1.49 Å. All corresponding bond lengths (distances) and bond angles are in good agreement except for the difference between dihedral angle of the two phenyl rings ($\theta_1$ = 139.8°), between the phenyl ring and oxazoline moiety ($\theta_2$ = −175.4°), and between oxazoline and hydroxamic acid ($\theta_3$ = −174.0°). The most interesting structural feature of molecule **32** is the rigidity of oxazoline moiety as well as flexibility between phenyl ring and oxazoline because the torsional angles $\theta_1$, $\theta_2$, and $\theta_3$ can twist from 0° to 360°. The brief analysis for calculations of the Gasteiger–Huckel charges for molecule **32** in the gas phase at the AM1 MOPAC level is shown in

Supplementary material 1, Fig. 1b. The results demonstrated that the partial negative charge was mainly concentrated at oxygens of the oxazoline ring and hydroxamic acid, whereas partial positive charges lay at the hydrogen directly bonded to oxygen atom of hydroxamic acid moiety. The rest of the molecules were built by changing the required substitution using optimized geometry of molecule **32** as the template and were minimized similarly.

MESP, Hydrogen bond donor/acceptor density analysis, and HOMO/LUMO studies are some of the approaches that can be used to study a molecule's electronic environment[8,9]. The knowledge of hydrogen bonding sites on a molecular surface is a powerful tool for ligand interaction with receptor studies. Ligands can be docked to proteins by matching the patterns displayed on the surface. Common density parameters on the LpxC inhibitors' surfaces are used to evaluate characteristic requirement for LpxC inhibitors by comparing potential region with molecule (i.e., molecule **32**).

Eq. 1 indicated that, hydrogen acceptor/donor density ($\rho_{acc/don}$) is calculated as follows: for every surface dot a sphere with a given cutoff radius is defined and the number of hydrogen acceptors and donors on the molecular surface inside this sphere ($\sum n_{acc/don}$) is counted. This number is divided by the enclosed surface area inside the sphere ($a_{total}$). If a hydrogen donor/acceptor is inside the cutoff sphere then $n_{acc/don} = 1$, if it is at the border of the cutoff sphere, only the surface part inside the sphere is considered, that is, $0 < n < 1$ and if it is completely out of the sphere $n_{acc/don} = 0$.

$$\rho_{acc/don(i)} = \frac{\sum_j n_{acc/don(j)}}{a_{total}} \tag{1a}$$

$$n_{acc/don} = \begin{cases} 1 \\ 0 \leqslant n \leqslant 1 \end{cases} \tag{1b}$$

where

$\rho_{acc/don(i)}$ = hydrogen acceptor/donor density ($\text{Å}^{-2}$) around surface dot.
$n_{acc/don(j)}$ = part of the hydrogen acceptor/donor $j$ which is inside the cutoff radius around surface dot $i$.
$a_{total}$ = surface area inside cutoff radius around surface dot $i$ ($\text{Å}^{-2}$).

All MESP and HD calculations and visualization were carried out using the MOLCAD program implemented in the SYBYL6.9 molecular modeling package. The Gasteiger–Huckel charges were assigned to the atoms of structures, and MESP and HD surfaces were generated and visualized.

An attempt to estimate the pharmacophoric features for LpxC inhibitors based on molecular electrostatic potential surfaces (MESP) and Hydrogen bond donor/acceptor density (HD) parameters was made (Figs. 1–3), by taking into consideration R-configuration at

4-position in ring. For clear understanding of how stereochemistry in molecule affects activity, we also calculated all parameters taking into consideration S-configuration at 4-position in ring. The brief data are shown in Supplementary material 2, Table 1a and b; Fig. 1a–d.

Bhattacharrjee and Karle have used the MESP to relate the anti-malarial potency of carbinolamine analogs[10] and neurotoxicity of artemisinin analogs[11] with corresponding structures. In the present study, MESP calculation on the LpxC inhibitors (Table 1) showed that these inhibitors were more potent when they possessed a large lateral positive potential region across the side chains at C4 and C5 of phenyl ring and hydroxamic acid. A negative potential adjacent to the carbonyl oxygen atom of hydroxamic acid and oxazoline ring has also been observed. Lack of negative potential regions over the phenyl ring indicates nucleophilic susceptibility of the phenyl ring plane. MESP plotted onto essentially the van der Waals surface of the molecules shows the site for the most negative potential and positive potential. The overall positive potential on the van der Waals surface of the molecule was observed to be in the range of 29.7–61.4 kcal/mol and the negative potential was in the range of −44.3 to −60.9 kcal/mol (Table 1).

Subsequently, functional correlation of different groups with the potency of the inhibitor was studied and a reasonable difference in the electronic properties was found. Three-dimensional iso-potential contours of MESP showed negative potential regions around the amide, nitrogen, hydroxyl, and F, $OCF_3$ groups. Disappearance of nearly all of the negative potential near phenyl ring and appearance of more positive potential at $OCH_3$, $CH_3$, and $OCH=CH_2$ (Fig. 1) indicates that this functional variation of groups around the phenyl ring and hydroxamic moiety has direct impact on the binding of inhibitors to LpxC binding site. These groups are also more hydrophobic in nature and demonstrated an increased efficacy of binding to LpxC.

Detailed analysis of the iso-contour of potentially high acting, intermediate acting, low acting, and inactive known inhibitors of LpxC on same scale (38.0 to −80.0 kcal/mol) showed characteristic difference in MESP values. In case of more potent inhibitors (compounds **32** and **5**), higher value of the positive potential (22.3–38.0 kcal/mol) with slight negative potential (−40.7 to −56.4 kcal/mol) around the phenyl ring (umbrella-shaped iso-contour) and presence of hydrophobic functionality (e.g., $OCF_3$ and –Ph–$CH_2$–$CH_2$) increase the hydrophobicity in active site and hydroxamic acid moiety makes hydrogen bonding with active site residue, which are chief determinants for activity and could be a reason for increased binding to LpxC. In case of intermediately acting inhibitors (compounds **29** and **31**) positive (22.3–30.1 kcal/mol) and negative (−24.9 to −40.7 kcal/mol) potential was observed around the phenyl ring along with decreased hydrophobicity which could be a reason for decrease in the potency of these inhibitors. However, 2-arylthiazolines class of inhibitors (compounds **76**–**81**) show intermittent
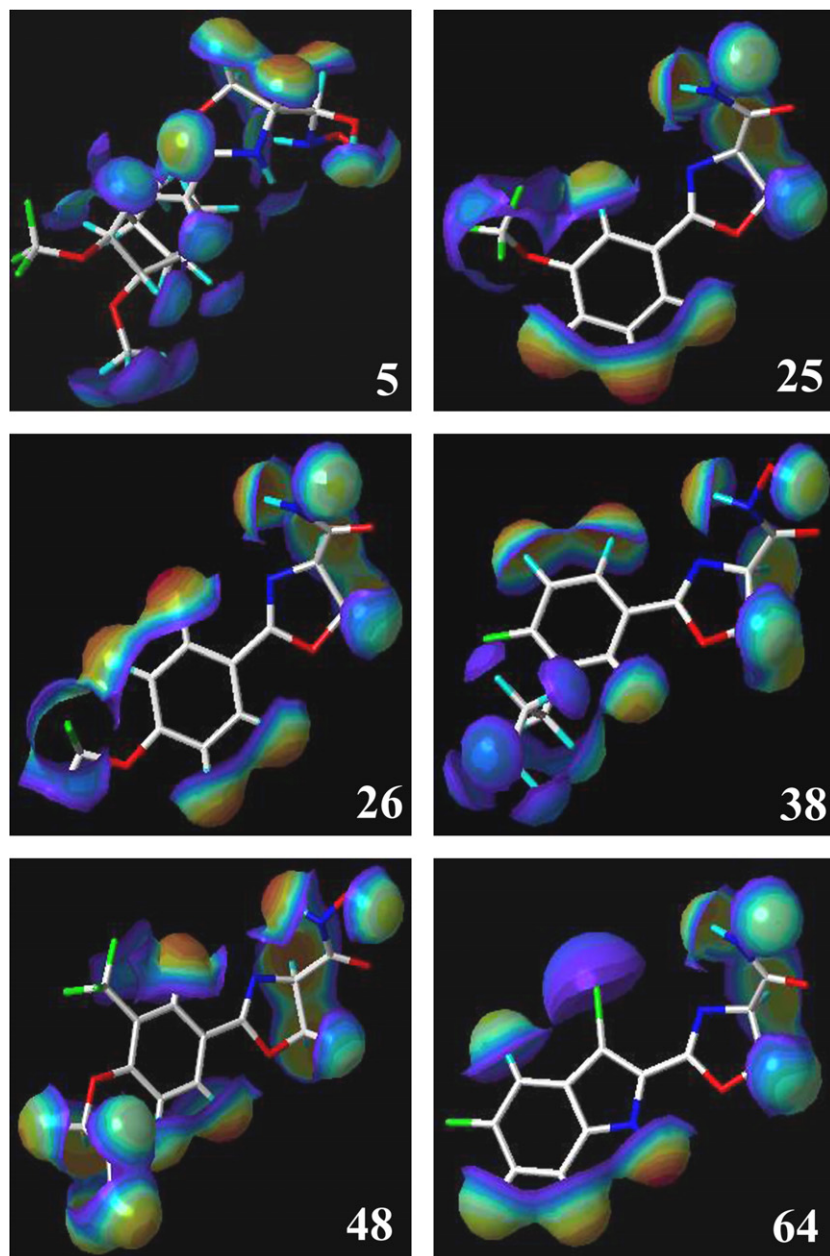
**Figure 1.** Three-dimensional iso-potential contours of MESP showing negative potential regions around the amide, nitrogen, hydroxyl, and OCF$_3$ groups. Disappearance of nearly all of the negative potential near phenyl ring and appearance of more positive potential at OCH$_3$, CH$_3$, and OCH=CH$_2$ is noticeable.

activity even with presence of hydrophobic functionality, this could mainly be due to replacement of oxazoline ring by thaizoline ring (Table 1), as carbonyl oxygen of oxazoline ring makes strong hydrogen bonding with active site residues.[12,13] Corresponding observations could be made with low activity inhibitors (compounds **67** and **77**) which showed increased positive potential (30.1–37.1 kcal/mol) around phenyl ring. A very striking observation in case of heterocyclic moiety containing inhibitors (compounds **58**–**62)** was that, the replacement of phenyl with heterocyclic aromatic groups at the 2-position of oxazoline varied the activity substantially. MESP also demonstrated a large difference in their negative potential (−56.4 to −72.1 kcal/mol) and increase in positive potential (30.1–38.0 kcal/mol) around phenyl

ring. The indole and 1*H*-indazole ring containing analogs are good inhibitors, whereas pyrazole moiety containing compounds **58** and **59** are inactive even on having largest negative potential in LpxC inhibitors series which otherwise seemed to be an essential feature for activity. One of the reasons that could be proposed is that they do not possess a large positive potential around the pyrazole moiety and hydrophobic functionality which is one of the requirements for the LpxC inhibitor activity is also absent. This overall observation is in agreement with the explanation reported by Kline et al. and Pirrung et al.[4,5]

Along with MESP analysis, common hydrogen bond acceptor/donor density parameters were used to

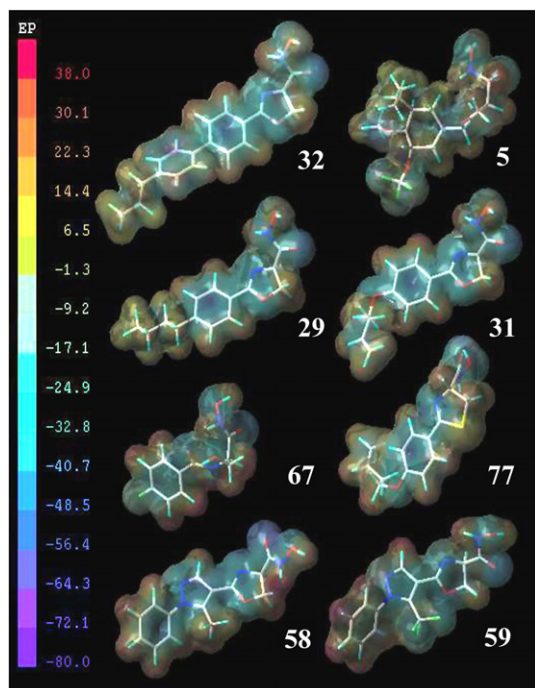**Figure 2.** Molecular electrostatic potential (MESP) surfaces property of the known inhibitors of the LpxC on same MESP scale. Molecules **32** and **5** indicate most active compounds in LpxC inhibitors series, molecules **29** and **31** indicate intermediately active compounds, molecules **67** and **77** indicate low activity compounds, and molecules **58** and **59** indicate strikingly inactive compounds in LpxC inhibitor series. (The color ramp for EP ranges from red (most positive; 38.0 kcal/mol) to purple (most negative; −80.0 kcal/mol).)

**Figure 3.** Hydrogen bond acceptor/donor density of the known inhibitors of the LpxC on same HD scale. Molecules **32** and **5** indicate most active compounds in LpxC inhibitors series, molecules **29** and **31** indicate intermediately active compounds, molecules **67** and **77** indicate low activity compounds, and molecules **58** and **59** indicate strikingly inactive compounds in LpxC inhibitor series. (The color ramp for HD ranges from magenta (high density; 0.056 e/au$^2$) to white (low density; 0.00 e/au$^2$).)

evaluate characteristic requirements for LpxC inhibitors (Table 1). Observations similar to MESP analysis were obtained from this study. The density ranges from high density (0.056) region to low density region (0.00). Compounds with varying activities have a very slight difference in their density maps (Fig. 3). All share common density region corresponding to hydroxamic acid region (0.049–0.056) (Supplementary material 3, Fig. 1). The overall density function indicates that potent inhibitors against LpxC need to have less density around the phenyl ring as observed for compounds **32** and **5** having HD value 0.015–0.022 and more density around the hydroxamic acid moiety (magenta color, umbrella-shaped iso-contours) which is making strong H$_2$-bonding and van der Waals interaction with active site pocket and novel zinc-binding motif characteristic of all known LpxC enzyme (Supplementary material 3, Fig. 1).

We have calculated LUMO and HOMO values for all molecules in the dataset (Table 2). Mechanistically, the electron acceptor ability of the LUMO may play a greater role than the electron donation of the HOMO. The HOMO eigenvalues are consistently highly negative <−8 kcal/mol, indicating that the electrons are firmly bound to the nuclei. The LUMO eigenvalues are also consistently negative, the most negative being −1.14 kcal/mol, which also indicates a strong affinity for electrons. The orbital energies of both HOMO and LUMO, which are the quantum-chemical descriptors correlated with various biological activities, were calcu-
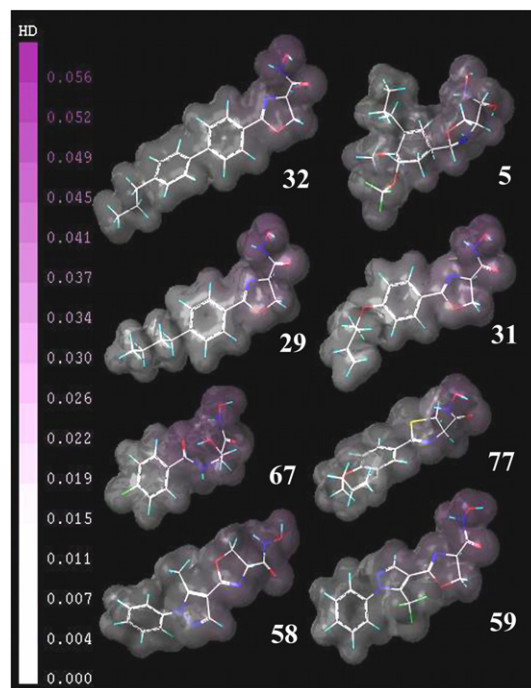
lated for all the molecules and are reported in Table 2. Nearly all molecules have a higher HOMO (−8.32 eV) and lower LUMO (−1.14 eV) energies. In particular, it was noted that the energy gap of HOMO–LUMO (HLG) of all potent molecules is more (−8.36 eV) except 35 and 38 than the corresponding HLG values of the intermediate and less potent or inactive molecules (−9.40 eV). More specifically, the HLG of all molecules is negative value which favors the distribution of electron density because HLG is a critical parameter determining the molecular admittance. It can be said that the larger the HLG value, the more stable the molecule and, thus, the harder (higher) the rearrangement of its electron density in the presence of an external charge or external electric field.[14] The HOMO–LUMO gap value results also support that presence of carbonyl oxygen loan pair at the hydroxamic acid and overall the distribution of HOMO and LUMO energies which are located in two distinct parts of the molecule are necessary for LpxC inhibitory activity. It can be seen that the HOMO and LUMO are π-like orbitals.[15] The HOMO electron density was primarily concentrated on the carbonyl oxygen part of hydroxamic acid, favoring a strong electrostatic or π–π stack interaction with the residues of the receptor mainly with Phe181 (This inference is part of docking study of LpxC inhibitors into homology model of LpxC; submitted elsewhere). On the other hand, the LUMO electron density primarily concentrated on the hydroxyl hydrogen of phenyl ring and phenyl counterpart in which the negatively charged polar residues of

**Table 2.** Lowest molecular orbital, highest molecular orbital, and dipole moment calculation of LpxC inhibitors

| Mol. I.D. | LUMO[a] | HOMO[a] | HLG[a] | Dipole moment[b] |
|---|---|---|---|---|
| 5 | −0.91 | −9.69 | −8.78 | 13.8 |
| 19b | −0.53 | −9.60 | −9.07 | 7.73 |
| 25 | −0.97 | −9.88 | −8.91 | 11.6 |
| 26 | −1.14 | −9.92 | −8.78 | 10.5 |
| 28 | −0.98 | −9.76 | −8.78 | 11.0 |
| 29 | −0.53 | −9.61 | −9.07 | 9.55 |
| 30 | −0.41 | −9.28 | −8.87 | 12.5 |
| 31 | −0.49 | −9.37 | −8.88 | 9.73 |
| 32 | −0.76 | −9.12 | −8.36 | 11.7 |
| 35 | −0.81 | −9.83 | −9.02 | 3.77 |
| 38 | −0.76 | −9.69 | −8.93 | 5.18 |
| 47 | −0.97 | −9.89 | −8.92 | 10.9 |
| 52 | −0.40 | −8.66 | −8.26 | 8.88 |
| 53 | −0.54 | −9.47 | −8.93 | 3.89 |
| 58 | −0.48 | −9.58 | −9.10 | 8.43 |
| 59 | −0.88 | −9.80 | −8.92 | 9.79 |
| 60 | −0.65 | −9.11 | −8.46 | 6.45 |
| 61 | −0.55 | −8.93 | −8.38 | 10.2 |
| 62 | 0.22 | −8.32 | −8.10 | 7.11 |
| 65 | −0.30 | −9.77 | −9.40 | 9.88 |
| 66 | −0.27 | −9.47 | −9.20 | 12.6 |
| 67 | −0.59 | −9.99 | −9.40 | 2.96 |
| 71 | −0.66 | −9.63 | −8.97 | 9.56 |
| 72 | −0.52 | −9.07 | −8.55 | 10.0 |
| 76 | −0.63 | −9.22 | −8.59 | 7.75 |
| 77 | −0.52 | −9.11 | −8.59 | 9.48 |
| 80 | −0.90 | −9.35 | −8.45 | 11.3 |
| 81 | −0.50 | −9.17 | −8.67 | 9.16 |

Note. HLG is (HUMO–LUMO).
[a] Indicate (eV) unit.
[b] Indicate (debye) unit.

the receptor are favorable. These results demonstrated that the HOMO and LUMO energy distribution on two distinct parts of the molecules is essential for inhibitor activity of all molecules in LpxC series.

The dipole moment of the compounds varies widely from 2.96 to 13.8 debye and these values have been correlated to long range ligand–receptor recognition and subsequent binding to LpxC. But this range does not have any apparent effect on LpxC inhibitory activity (Table 2).

This study showed that potent LpxC inhibitors share specific molecular electronic properties regardless of phenyl ring environment or the occurrence of cyclic or acyclic moieties. The values of the MESP by the hydroxyl, nitrogen, and carbonyl oxygen groups, and the shape and distribution of the iso-potential surfaces of all the compounds in this study are essentially the same as those found in the most potent LpxC inhibitors.[4] Thus, LpxC inhibitors whose negative potential ranges from −49.8 to −59.3 kcal/mol, positive potential is at least 32.6 kcal/mol, and which have a laterally extended negative potential region adjacent to, but not over the phenyl ring system, should be relatively potent LpxC inhibitors. These calculable values provide a guide to the chemist as to which compounds are worthy of expensive chemical synthesis. To confirm the goodness of our findings, we evaluated the reported series of PDE4 and TNF-α inhibitors proposed as the metallo-

enzyme target inhibitors.[16,17] The observations for these molecules were in consistence with the observations reported in this paper, thereby, proving that the features observed to be responsible for LpxC inhibition in this study are in fact relevant and are applicable to a wider range if ligands are not restricted to the class of molecules studied. (The detailed analysis is given in Supplementary material 4, Table 1; Fig. 1). Particular electronic properties, that is, MESP, hydrogen bond acceptor/donor, and HUMO/LUMO values, etc. indicate that inter-molecular hydrogen bonding is an important element in the interaction of the LpxC inhibitors with its binding site. MESP properties include the location of the most positive potential and intermediate HD at side-chain groups of LpxC inhibitors like $OCH_3$, $CH_3$, and $OCH=CH_2$. The large negative potential and high HD located on the groups like F, $OCF_3$, and carbonyl oxygen atom of hydroxamic acid and oxazoline ring. There is a disappearance of nearly all of the negative potential near phenyl ring. This overall distribution of MESP property gives a measure of strength of hydrogen bonding of LpxC inhibitors in the range of 32.6–61.4 kcal/mol. The relative electrophilicity of the phenyl ring also appears to be important for LpxC inhibitory potency. Lack of negative potential regions above the phenyl ring is associated with LpxC inhibitory potency suggesting a requirement for interaction with electron-rich regions of the receptor. The large potential surfaces extending from the molecule lateral to the phenyl ring may be an important recognition element for the receptors. These large, extended negative potential regions are an indication of regions with higher electron density and are likely to enhance the hydrophobicity/lipophilicity of the compounds. The hydrophobicity has been shown to be an important contributing factor toward potent LpxC inhibitor activity.

Substitution of electron-withdrawing groups like $OCF_3$, $CF_3$, F, and $OCH=CH_2$ groups or halogens in the phenyl ring in the compounds facilitates the decrease in negative potential at the rings and also increases the hydrophobicity lateral to the phenyl ring. When the compounds in this study were grouped by the heterocyclic/non-heterocyclic nature, no significant relationships between amine group type and electronic properties were found except in compounds **58** and **59**. This difference in the electrostatic profiles of **58** and **59**, which have a highest negative potential region extending from the hydroxyl group to the nitrogen of oxazoline ring, from the rest of the compounds may indicate a different recognition interaction with receptors and a different manner in which these bind to receptors.

The findings of this study shall be useful in designing new more potent *P. aeruginosa* deacetylase LpxC inhibitors. This can be achieved by incorporating such structural features into the ligands that modify the electronic properties in accordance with the results of this work. The methodology employed in this study for calculating molecular electronic properties, correlating these properties to biological potency, and compiling a set of electronic properties that are necessary for potent biological activity should be applicable to other classes of

compounds, enabling educated decisions on the design of new compounds.

## Supplementary data

Supplementary data associated with this article can be found, in the online version, at doi:10.1016/j.bmcl.2006.11.069.

## References and notes

1. Nicoll, L. *N. Eng. J. Med.* **1995**, *332*, 616.
2. Van Delden, C.; Iglewski, B. H. *Emerg. Infect. Dis.* **1998**, *4*, 551.
3. Whittington, D. A.; Rusche, K. M.; Shin, H.; Fierke, C. A.; Christianson, D. W. *Proc. Natl. Acad. Sci. U.S.A.* **2003**, *100*, 8146.
4. Kline, T.; Andersen, N. H.; Harwood, E. A.; Bowman, J.; Malanda, A.; Endsley, S.; Erwin, A. L.; Doyle, M.; Fong, S.; Harris, A. L.; Mendelsohn, B.; Mdluli, K.; Raetz, C. R.; Stover, C. K.; Witte, P. R.; Yabannavar, A.; Zhu, S. *J. Med. Chem.* **2002**, *45*, 3112.
5. Pirrung, M. C.; Tumey, L. N.; Raetz, C. R.; Jackman, J. E.; Snehalatha, K.; McClerren, A. L.; Fierke, C. A.; Gantt, S. L.; Rusche, K. M. *J. Med. Chem.* **2002**, *45*, 4359.
6. SYBYL; version 6.9; Tripos Associates Inc.; 1699, S Hanley Rd., St. Louis, MO631444; USA.
7. Dewar, M. J.; Zoebisch, E. G.; Healy, E. F.; Stewart, J. P. *J. Am. Chem. Soc.* **1985**, *107*, 3902.
8. Murray, J. S.; Zilles, B. A.; Jayaswuya, K.; Politzer, D. *J. Am. Chem. Soc.* **1986**, *108*, 915.
9. Naray-Szabo, G. *J. Mol. Graphics* **1989**, *7*, 76.
10. Bhattacharrjee, A. K.; Karle, J. M. *Bioorg. Med. Chem.* **1998**, *6*, 1927.
11. Bhattacharrjee, A. K.; Karle, J. M. *Chem. Res. Toxicol.* **1999**, *12*, 422.
12. Whittington, D. A.; Rusche, K. M.; Shin, H.; Fierke, C. A.; Christianson, D. W. *Proc. Natl. Acad. Sci. U.S.A.* **2003**, *100*, 8146.
13. Clure, C. P.; Rusche, K. M.; Peariso, K.; Jackman, J.; Fierke, C. A.; Penner-Hahn, J. E. *J. Inorg. Biochem.* **2003**, *94*, 78.
14. Robert, G. P.; Ralph, G. P. *J. Am. Chem. Soc.* **1983**, *105*, 7512.
15. Cao, H.; Pan, X.-L.; Li, C.; Zhou, C.; Deng, F.-Y.; Li, T.-H. *Bioorg. Med. Chem. Lett.* **2003**, *13*, 1869.
16. Kleinman, E. F.; Campbell, E.; Giordano, L. A.; Cohan, V. L.; Jenkinson, T. H.; Cheng, B.; Shirley, J. T.; Pettipher, E. R.; Salter, E. D.; Hibbs, T. A.; DiCapua, F. M.; Bordner, J. *J. Med. Chem.* **1998**, *41*, 266.
17. Pirrung, M. C.; Tumey, L. N.; McClerren, A. L.; Raetz, C. R. H. *J. Am. Chem. Soc.* **2003**, *125*, 1575.